Molecular Therapy
Methods & Clinical Development
Original Article

STRIP2 Is Indispensable for the Onset of Embryonic Stem Cell Differentiation

Davood Sabour,[1,5] Sureshkumar Perumal Srinivasan,[1] Susan Rohani,[1] Vilas Wagh,[1,4] John Antonydas Gaspar,[1] Darius Panek,[1] Mostafa Abootorabi Ardestani,[2] Michael Xavier Doss,[1] Nicole Riet,[3] Hinrich Abken,[3] Jürgen Hescheler,[1] Symeon Papadopoulos,[2] and Agapios Sachinidis[1]

[1]Institute of Neurophysiology and Center for Molecular Medicine Cologne (CMMC), University of Cologne (UKK), Robert-Koch-Strasse 39, 50931 Cologne, Germany; [2]Institute of Vegetative Physiology, Center of Physiology and Pathophysiology, University of Cologne, Robert-Koch-Strasse 39, 50931 Cologne, Germany; [3]Department I for Internal Medicine, Center for Molecular Medicine Cologne, Robert-Koch-Strasse 21, University of Cologne, and University Hospital Cologne, 50931 Cologne, Germany

The role of striatin interacting protein 2 (Strip2) in differentiation of embryonic stem cells (ESCs) is still under debate. Strip2-silenced murine (KD) ESCs were differentiated for 4, 8, 12, and 16 days. We show that Strip2 is distributed in the perinucleus or nuclei of wild-type (WT) undifferentiated ESCs, but is localized in high-density nuclear bodies in differentiated cells. CellNet analysis of microarray gene expression data for the KD and scrambled control (SCR) embryoid bodies (EBs), as well as immunostainings of key pluripotent factors, demonstrated that differentiation of KD ESCs is repressed. This occurs even in 16-day-old EBs, which possessed a high tumorigenic potential. Correlated with very high expression levels of epigenetic regulator genes, *Hat1* and *Dnmt3*, enzymatic activities of the histone acetyltransferase type B (Hat1) and DNA (cytosine-5)-methyltransferase 3 beta (Dnmt3b) were higher in differentiated 16-day-old KD EBs than in SCR or WT EBs. The expression levels of let-7, 290, and 302 microRNA families were opposed in KD ESCs, while KD EBs had levels comparable to WT and SCR ESCs during differentiation. Strip2 is critical for the regular differentiation of ESCs. Moreover, Strip2 deficient ESCs showed a dysregulation of epigenetic regulators and microRNAs regulating pluripotency.

INTRODUCTION

Recently, increasing attention has been directed toward identifying and understanding the function and intracellular signaling pathways of the striatin-interacting phosphatase and kinase (STRIPAK) complex in regulating biological processes of multiple organisms.[1–3] There is growing evidence that striatin interacting protein 2 (Strip2; also known as Fam40b) is a member of the STRIPAK complex, which may be involved in the regulation of cell growth, proliferation, cell migration and adhesion, neural and vascular development, and ultimately may regulate cardiac function.[1–3] Striatin, a core of the STRIPAK complex, is highly expressed in the central and peripheral nervous systems, in heart muscle, testes, and lymphocytes.[3] Thus, Striatin and Strip2 may play important roles in several biological processes, such as differentiation, cell growth, development differentiation, and cancer.[4] More recently, it has been shown that Strip2 plays an important role in cancer development and metastasis.[5] Previously, we provided evidence that Strip2 is required for proper differentiation of embryonic stem cells (ESCs). In this context, we have shown that short hairpin RNAs (shRNAs) mediated silencing of Fam40b expression in ESCs led to perturbed differentiation to different somatic cell types at 12-day embryoid bodies (EBs), including a complete abrogation of cardiomyogenesis. Interestingly, pluripotency factors, such as *Nanog*, *Oct4*, and *Sox2*, as well as epigenetic factors, such as histone acetyltransferase type B (Hat1) and DNA (cytosine-5)-methyltransferase 3b (Dnmt3b), were highly upregulated in Strip2-silenced 12-day EBs (KD EBs), compared with scrambled control (SCR) EBs. We identified the gene product of *Strip2* in undifferentiated ESCs, as a nuclear and perinuclear protein, with a molecular weight of 96 kDa.[6] To prove that Strip2 is essential for differentiation of ESCs toward defined somatic cells, and to determine its underlying mechanisms, we extended our study by performing detailed parallel transcriptome and microRNA (miRNA) expression studies following differentiation of KD, SCR, and wild-type (WT) ESCs for periods of 4, 8, 12, and 16 days. The cell types differentiated from KD, SCR, and WT ESCs have been classified, using the online CellNet bioinformatics platform (http://cellnet.hms.harvard.edu/run/). In addition, the activities of the epigenetic regulators Hat1 and Dnmt3b have been investigated during differentiation of the KD and SCR ESCs. Here, we show that Strip2 is located in differentiated cells, in dense nuclear bodies, demonstrating that Strip2 is a key nuclear factor, acting during the very early stages to differentiate all three germ layers. Moreover, Strip2 regulates the activity of the nuclear epigenetic regulators Hat1 and Dnmt3b and the expression of a set of miRNAs

Received 7 April 2017; accepted 11 April 2017;
http://dx.doi.org/10.1016/j.omtm.2017.04.001.

[4]Present address: Massachusetts General Hospital, 55 Fruit Street, Boston, MA 02114, USA

[5]Present address: Department of Genetics, Faculty of Medicine, Babol University of Medical Sciences, 47134 Babol, Iran

Correspondence: Professor Dr. Agapios Sachinidis, University of Cologne (UKK), Institute of Neurophysiology and Center for Molecular Medicine Cologne (CMMC), Robert-Koch-Strasse 39, 50931 Cologne, Germany.
E-mail: a.sachinidis@uni-koeln.de

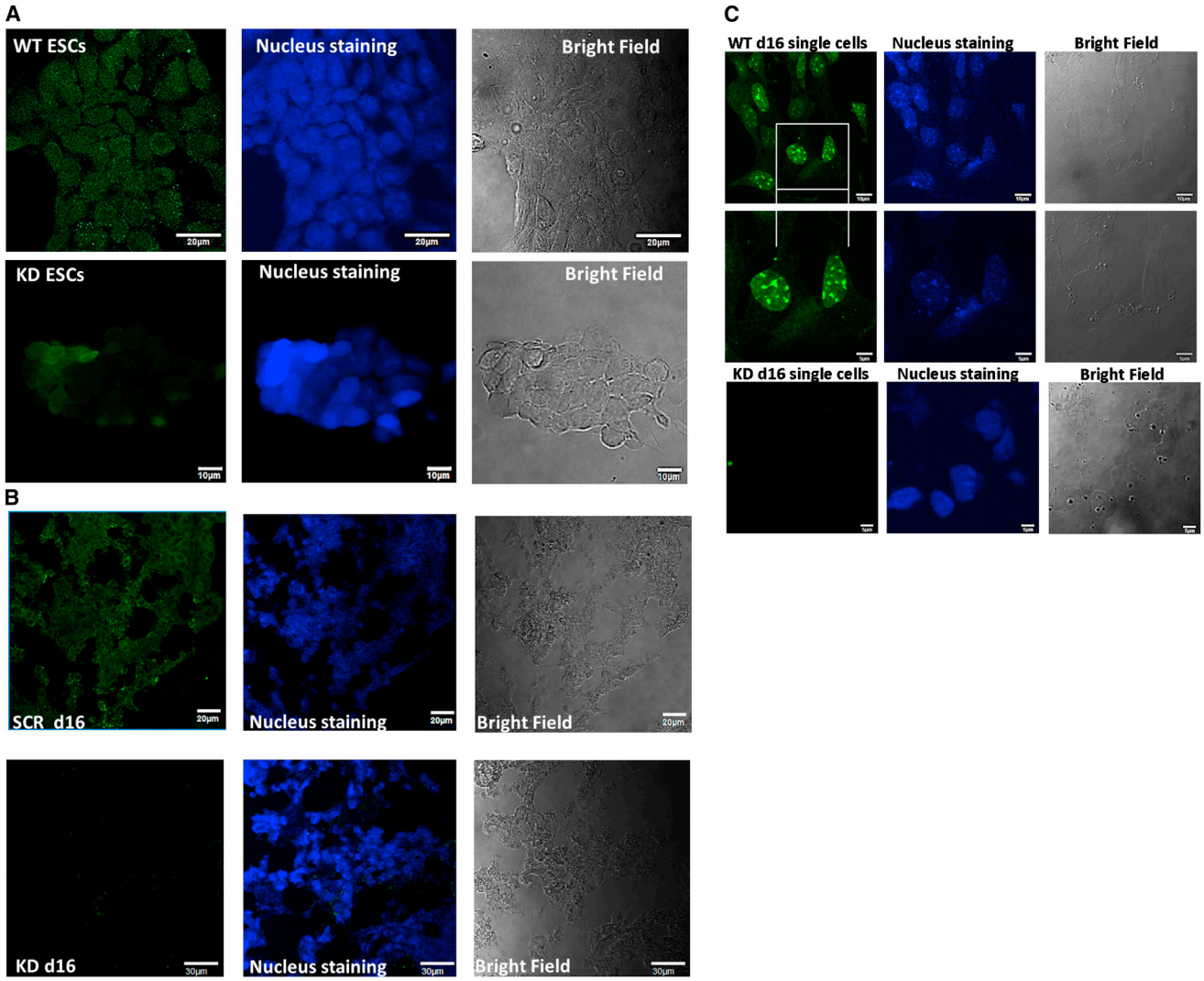

Figure 1. Cellular Localization of Strip2

(A) Strip2 expression in WT, and Strip2-silenced KD ESCs. (B) Strip2 expression in cryosections of the 16-day SCR and KD EBs. (C) Detection of Strip2 in differentiated single cells generated after trypsinization of 16-day-old EBs, with further culturing for 24 hr. The protein was mainly located in nuclear bodies of some, but not all 16-day differentiated cells. Immunostaining of Strip2 was performed using primary anti-Strip2 antibodies (sc-162799; 1:200) and donkey anti goat IgG-FITC secondary antibody (sc-2024, 1:200), as a secondary antibody (upper scan; green pseudo color). The cells were co-stained with the nuclear marker Hoechst 33342 (middle scan; blue pseudo color). The overlay of nuclear and Strip2-staining (bottom scan) reveals that the presence of Strip2 is not restricted to the nucleus, but also extends to perinuclear or even cytoplasmic domains of the ESCs (dimensions of scale bars are indicated in each image).

required for switching the pluripotency state of the ESCs to a differentiation state.

RESULTS

Detection of Strip2 in Differentiated ESCs

Using a Strip2 (Fam40b) shRNA expression vector targeting mouse Strip2 and a scrambled shRNA control vector with a non-active scrambled sequence cassette, we previously generated a constitutive Strip2 KD ESC line. In this cell line, Strip2 was constitutively knocked down (referred to as KD ESCs) in mRNA and protein levels, as well as in SCR ESCs.[6] Here, we also use control WT ESCs for our comparative investigations. Strip2 detection by immunostaining in undifferentiated and differentiated KD and SCR ESCs is shown in Figure 1A. Strip2 was sporadically distributed within the nuclei of the undifferentiated ESCs. No significant expression could be observed in the nuclei of the KD ESCs. Figure 1B shows that Strip2 was intensely detected in several areas of the EBs, consisting of several somatic cell types. No significant expression could be detected in the 16-day-old KD EBs (Figure 1B). Detection of Strip2 in differentiated single cells, generated after trypsinization of 16-day-old EBs and further culturing

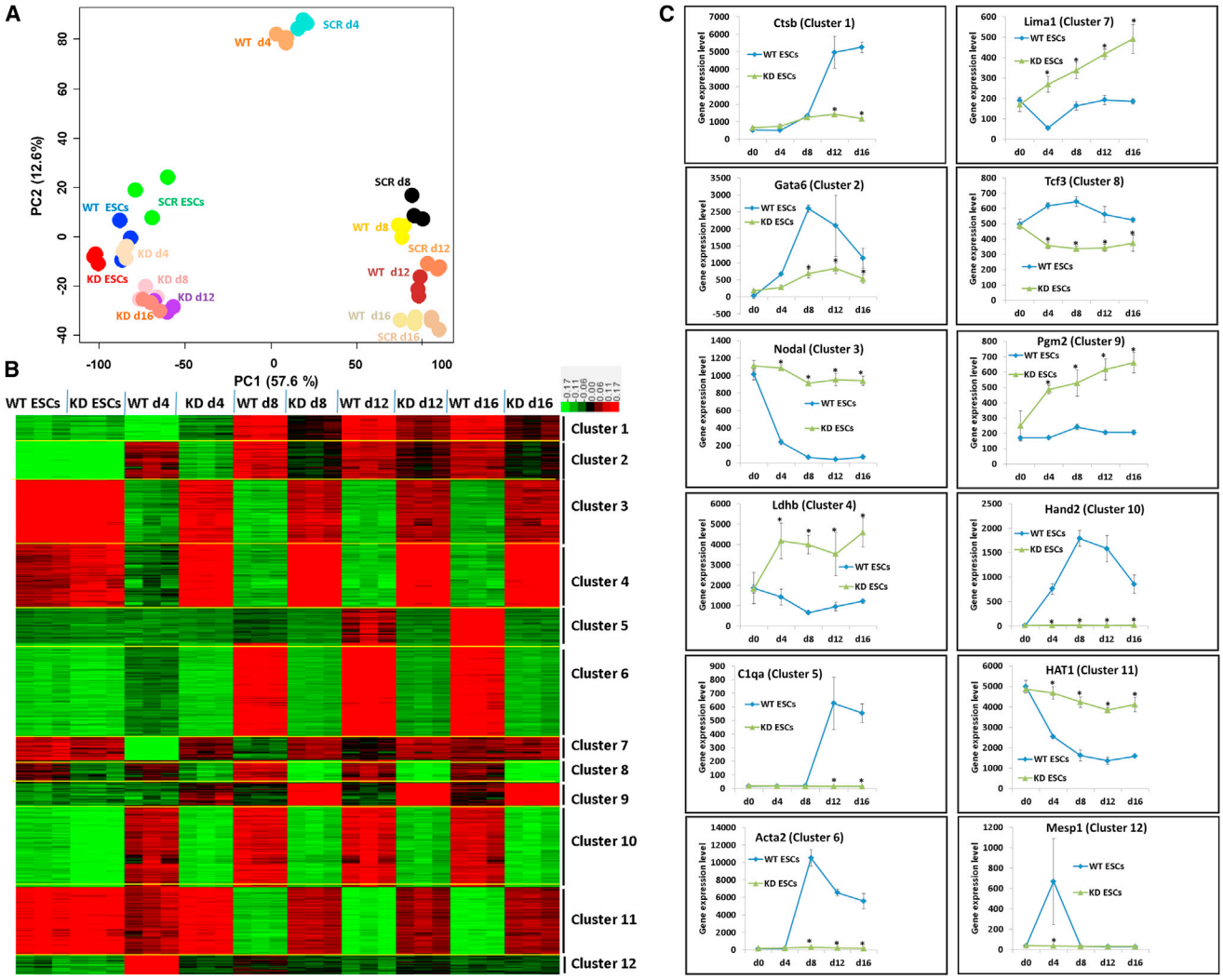

Figure 2. Transcriptome Analysis of Undifferentiated and Differentiated Strip2 KD, Control SCR, and WT ESCs

Differentiation of these cells was performed for 4-, 8-, 12-, and 16-day periods. (A) PCA of genome-wide gene expression. Each sphere represents an individual sample from a color-coded triplicate sample set. (B) Visualization of K-means clustering of 10,548 differentially expressed probe sets (with at least a 2-fold change in expression), using a Euclidean distance measurement and k = 12 group clusters. The replicates are displayed on the vertical axis, with genes on the horizontal axis. Log2 transformed signal intensities are depicted, using a color gradient. The heatmap indicates high expression levels in red, intermediate expression in dark gray, and low expression levels in green. (C) Representative diagrams showing the gene expression pattern of various clusters of genes during differentiation of KD and WT ESCs (*$p < 0.05$ for the differentiated KD versus WT ESCs, mean ± SD, n = 3). (D) Validation of the microarray data by the real-time qPCR analysis of six genes (*$p < 0.05$ for differentiated KD ESCs versus SCR ESCs, mean ± SD n = 3).

for 24 hr, is shown in Figure 1C. Results suggest that Strip2 is located in nuclear bodies of the 16-day-old differentiated cells, but was absent in the 16-day-old KD EBs.

Analysis of Differentially Expressed Genes

In our previous study, KD, SCR, and WT ESCs were differentiated for 12 days (12-day-old EBs), using the hanging drop protocol, and their transcriptomes were characterized.[6] Transcriptome characterization of the undifferentiated KD ESCs and the 12-day-old EBs indicated that Strip2 was essential for the differentiation of ESCs into somatic cells present in 12-day-old EBs via mechanisms controlling pluripotency. However, our findings did not allow us to determine whether Strip2 was required for the development of germ layers from ESCs or for the development of somatic cells from germ layer cells. To answer this question, we extended our transcriptome studies by performing a similar study, including early (4-day), late (8-day and 12-day), and very late (16-day) differentiation stages of the KD, SCR, and WT ESCs and carrying out a detailed transcriptome analysis of these stages. In parallel, a miRNA expression analysis was performed, with the same total RNA. In

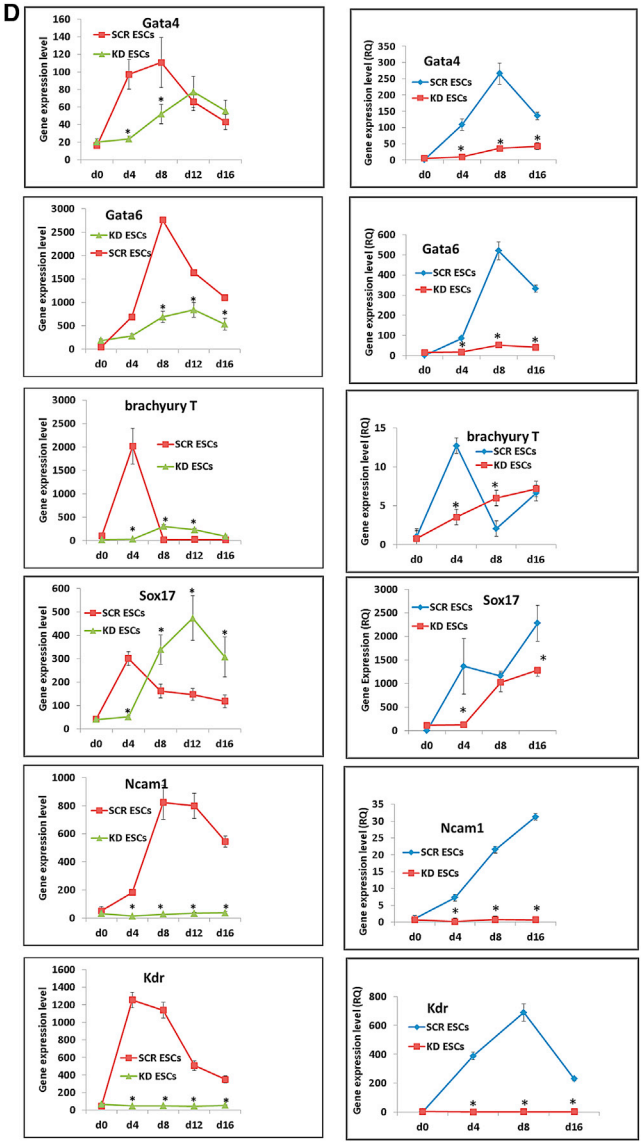

Figure 2. continued

general, 12,156 as well as 12,440 differentially expressed genes (at least 2-fold) have been identified in WT as well as in SCR 4-day (d4), 8-day (d8), 12-day (d12), and 16-day (d16) EBs in comparison to WT ESC (d0) as well as SCR ESCs (d0), respectively. In contrast, only 4,075 genes were found to be differentially expressed in KD d4, d8, d12, and d16 EBs in comparison to the KD ESCs (d0). Significance of the variance in expression levels in undifferentiated (KD, SCR, and WT ESCs) and in their respective differentiated 4-day, 8-day, 12-day, and 16-day-old EBs were evaluated using a principal component analysis (PCA) (Figure 2A). PC 1 shows the highest variance in transcriptome variability among these biological samples, followed by variation in PC2. As shown in Figure 2A, there are relatively large differences in the transcriptomes of all three cell populations. Briefly, PCA indicated that the transcriptomes of the undifferentiated KD, SCR, and WT ESCs were very similar, while they were significantly different from the transcriptomes of the differentiated SCR and WT (4-, 8-, 12-, and 16-day-old EBs). As expected, the transcriptomes of the differentiated SCR and WT (4-, 8-, 12-, and 16-day EBs) were very similar. Among them, the transcriptomes of the 4-day-old SCR and WT EBs (clustered together) differ significantly in their PC1 and PC2 weightings, compared with the transcriptomes of 8-, 12-, and 16-day-old EBs. These later stages show only small differences in PC2. Notably, the transcriptomes of the KD 4-, 8-, 12-, and 16-day-old EBs were similar to the transcriptomes of undifferentiated KD, SCR, and WT ESCs, having only small differences in PC2. There were 12 transcriptome clusters of different cell populations that were identified using the K-means clustering algorithm. These represent transcripts that were significantly deregulated among the different cell types (at least a 2-fold change) (Figure 2B). These clusters comprise genes (Table S1) that were similarly regulated during the differentiation of the KD, SCR, and WT ESCs. Figure 2C shows representative gene expression levels of the genes in these clusters (Table S1) during differentiation of the WT and KD ESCs. As shown in Figure S1A, the expression levels of the genes in differentiated SCR ESCs were very similar to the expression levels in the differentiated SCR ESCs. To categorize the biological significance of the differentially expressed genes, the Database for Annotation, Visualization and Integrated Discovery (DAVID) was used (https://david.ncifcrf.gov/). DAVID assigns a biological process, molecular function, and cellular component, based on a statistical enrichment score. The main developmental/differentiation associated Gene Ontology (GO) and Kyoto Encyclopedia of Genes and Genomes (KEGG) pathways for biological processes identified in the annotation enrichment analysis for all 12 clusters are shown in Table 1. The complete GO and KEGG pathways for all clusters are given in Table S2. Our detailed cluster analysis using DAVID indicated that clusters 3, 11, and 12 are of particular interest (Table 1). In cluster 3, 521 probe sets (PSs) (421 genes) have been identified. Interestingly, among them, the GO:0019827 stem cell maintenance ($p < 2.55 \times 10^{-8}$) and GO:0045596 negative regulation of cell differentiation ($p < 1.37 \times 10^{-4}$) were highly enriched. The GO:0019827 stem cell maintenance category includes several pluripotency-associated genes (*Nanog*, *Rif1*, *Esrrb*, *Pou5f1*, *Nodal*, *Sox2*, *Klf4*, *Fgf4*, and *Tcl1)*. Figure S2 shows that the expression level of these genes is maximal in an undifferentiated state, while during differentiation of WT and SCR, a rapid downregulation of the pluripotent genes began on day 4, continuing until day 16 (e.g., as seen in genes *Pou5f1*, *Nodal*, and *Sox2*). In striking contrast, the level of the pluripotent genes remained high during differentiation of the KD ESCs, after up to 16 days of differentiation (Figure S2). In cluster 12, 173 PSs (157 genes) have been identified. Among them, the GO:0001704 formation of primary germ layers (ectoderm, mesoderm, and endoderm) was highly enriched ($p < 4.15 \times 10^{-11}$) (Table 1). This GO set includes *Bmp4*, *Hand1*, *Lhx1*, *Eomes*, *Lef1*, *Smad1*, *Bmp7*, *Mesp1*, *Mixl1*, and *Bmpr1a*. As expected, the GO:0001707 mesoderm formation ($p < 2.00 \times 10^{-8}$; *Bmp4*, *Hand1*, *Eomes*, *Lef1*, *Smad1*, *Bmp7*, *Mesp1*, and *Bmpr1a*), the

Table 1. Specific GO and KEGG Pathways of the Cluster Specific Genes Indicated in Figure 2

GO and KEGG	Gene No.	p Value
Cluster 1		
GO:0006665 sphingolipid metabolic process	6	0.007178
GO:0006643 membrane lipid metabolic process	6	0.008196
mmu04144:Endocytosis	11	0.008332
mmu00603:Glycosphingolipid biosynthesis	3	0.032475
Cluster 2		
GO:0007167 enzyme linked receptor protein signaling pathway	20	7.38×10^{-5}
GO:0048514 blood vessel morphogenesis	15	5.55×10^{-4}
mmu04360:Axon guidance	9	0.009831
mmu04310:Wnt signaling pathway	9	0.020142
Cluster 3		
GO:0006520 cellular amino acid metabolic process	28	6.93×10^{-9}
GO:0019827 stem cell maintenance	9	6.51×10^{-8}
GO:0045596 negative regulation of cell differentiation	15	0.005
mmu00330:Arginine and proline metabolism	10	9.33×10^{-5}
Cluster 4		
GO:0006281 DNA repair	23	1.23×10^{-4}
GO:0019318 hexose metabolic process	19	2.06×10^{-4}
mmu00030:Pentose phosphate pathway	9	2.68×10^{-6}
mmu00480:Glutathione metabolism	11	1.56×10^{-5}
Cluster 5		
GO:0002526 acute inflammatory response	22	5.67×10^{-16}
GO:0009888 tissue development	40	3.31×10^{-7}
mmu04610:Complement and coagulation cascades	22	9.89×10^{-15}
mmu00980:Metabolism of xenobiotics by cytochrome P450	13	1.13×10^{-6}
Cluster 6		
GO:0009888 tissue development	84	6.31×10^{-13}
GO:0009887 organ morphogenesis	73	6.56×10^{-10}
mmu04512:ECM-receptor interaction	20	1.42×10^{-7}
mmu05414:Dilated cardiomyopathy	21	1.65×10^{-7}
Cluster 7		
GO:0042981 regulation of apoptosis	24	1.40×10^{-4}
GO:0043067 regulation of programmed cell death	24	1.68×10^{-4}
mmu04142:Lysosome	10	3.92×10^{-4}
mmu03320:PPAR signaling pathway	7	0.003697
Cluster 8		
GO:0043229 intracellular organelle	163	8.06×10^{-8}
GO:0005634 nucleus	98	4.50×10^{-6}
mmu04810:Regulation of actin cytoskeleton	10	0.003562664
mmu04520:Adherens junction	6	0.004405387

Table 1. *Continued*

GO and KEGG	Gene No.	p Value
Cluster 9		
GO:0030500 regulation of bone mineralization	5	7.73×10^{-5}
GO:0004867 serine-type endopeptidase inhibitor activity	9	4.52×10^{-4}
mmu04142:Lysosome	11	4.68×10^{-5}
Cluster 10		
GO:0009887 organ morphogenesis	69	8.67×10^{-12}
GO:0007507 heart development	36	3.63×10^{-10}
mmu04360:Axon guidance	24	3.32×10^{-9}
mmu04340:Hedgehog signaling pathway	14	2.19×10^{-7}
Cluster 11		
GO:0005730 nucleolus	84	1.72×10^{-49}
GO:0034470 ncRNA processing	42	4.05×10^{-24}
GO:0030529 ribonucleoprotein complex	57	1.06×10^{-15}
GO:0040029 regulation of gene expression, epigenetic	9	0.003
GO:0022618 ribonucleoprotein complex assembly	5	0.033
GO:0031080 Nup107-160 complex	7	5.70×10^{-8}
GO:0005643 nuclear pore	13	1.04×10^{-6}
GO:0051028 mRNA transport	13	1.90×10^{-6}
Cluster 12		
GO:0001704 formation of primary germ layer	10	4.15×10^{-11}
GO:0001707 mesoderm formation	8	2.00×10^{-8}
GO:0007492 endoderm development	5	1.06×10^{-4}
GO:0007398 ectoderm development	7	0.001

GO:0007492 endoderm development ($p < 1.06 \times 10^{-4}$; *Lhx1*, *Eomes*, *Cfc1*, *Mixl1*, and *Bmpr1a*), and the GO:0007398 ectoderm development ($p < 0.0010$) were also highly enriched (Table 1). In Figure 2C, like *Mesp1*, genes in cluster 12 show maximal expression levels only on day 4 in differentiated WT and SCR ESCs, but have low levels in undifferentiated cells (d0), as well as 8-, 12-, and 16-day-old EBs. Interestingly, the expression levels of these genes in KD ESCs were very low at all stages of differentiation, even in 4-day-old EBs (Figure 2).

In cluster 11, 842 PSs (676 genes) have been identified. Among them, genes encoding for nucleus proteins (GO:0005730 nucleolus; $p < 1.72 \times 10^{-49}$), non-coding (nc)RNAs processing genes (GO:0034470 ncRNA processing; $p < 4.05 \times 10^{-24}$), ribonucleoproteins (GO:0030529 ribonucleoprotein complex; $p < 1.06 \times 10^{-15}$), and RNA polymerases (KEGG, mmu03020:RNA polymerase; $p < 2.07 \times 10^{-4}$) were highly enriched. Genes participating in the regulation of gene expression via epigenetic mechanisms (GO:0040029 regulation of gene expression, epigenetic; $p < 0.0037$; *Tarbp2*, *Dnmt3a*, *Hat1*, *Lin28a*, *Dnmt3b*, *Sirt1*, *Mphosph8*, *Brca1*, and *Hells*) were also highly enriched. In Figure 2C, similar to expression

levels of *Hat1*, the expression levels of cluster 11 genes was maximal in their undifferentiated state in all three ESCs lineages. During differentiation of WT and SCR ESCs, a rapid downregulation of genes occurred from their undifferentiated state through 4-day- to 16-day-old EBs. In contrast, the expression levels of genes remained high during differentiation of KD ESCs until day 16 of differentiation (Figure 2C). Genes in clusters 5, 6, 8, and 10 were downregulated at all stages of differentiation of KD ESCs, as well as in 16-day-old KD EBs comprising somatic cell type specific genes of all lineages, including cardiac cells, kidney, neurons, liver cells, and blood cells (Table S2). In contrast, expression of clusters 5 and 6 genes in WT and SCR ESCs began on day 12 and day 8 of differentiation, respectively. Their expression levels remained high even on day 16 of differentiation. Similarly, in both WT and SCR ESCs, expression levels of the genes in cluster 8 and 10 began on day 4, with maximal expression occurring on day 8 of differentiation, while still high expression levels were observed on day 12 and 16 of differentiation. Clusters 1 and 2 genes were downregulated in KD ESCs during differentiation, compared with SCR and WT ESCs. These genes belong mainly to metabolic and organ developmental processes, respectively. Cluster 4 genes showed upregulation in differentiated KD ESCs, compared with differentiated SCR and WT ESCs. These genes belong mainly to metabolic processes (Figure 2; Table S2). The expression of mainly apoptosis-related genes in Cluster 7 increased during differentiation of KD ESCs, compared with differentiated SCR and WT ESCs (Figure 2; Table S2). Validation of the microarray data has been performed by real-time qPCR analysis of six genes involved into the germ layer formation and their cell derivatives (*Ncam1*: ectoderm, neurogenesis; *Brachyury T*: mesoderm, cardiomyogenesis; *Kdr*: mesoderm, hematopoietic stem cells; *Sox17*: endoderm, endoderm derived organs such as gut; and *Gata4* and *Gata6*: mesoderm and extraembryonic endoderm lineages, cardiomyogenesis, hepatogenesis) (Figure 2D). As shown, the microarray gene expression patterns of all six genes could be confirmed by the real-time qPCR method. Moreover, the expression levels in differentiated KD ESCs were significantly lower in comparison to the SCR ESCs at least at day 4 of differentiation. Overall, analysis suggests that Strip2 is essential for early differentiation of ESCs to germ layer cell types.

Cellular Identity of Various Differentiated ESCs

To distinguish the specific cell types differentiated from KD, SCR, and WT ESCs within a 16-day period, we uploaded their gene expression data (.CEL files) to the CellNet bioinformatics platform, available at http://cellnet.hms.harvard.edu/run/. As described,[7] such analysis allows prediction of the cell and tissue types, based on the cell and tissue specific gene expression levels derived from microarray gene expression data. The two main outputs of CellNet analysis are: (1) the cell versus tissue cell (C/T) classification score and (2) the C/T gene regulatory network (C/T GRNs) score. The values of the C/T classification score reflect the probability that a sample is indistinguishable from a given cell or tissue type based on its gene expression levels. These scores are typically represented as a heatmap, using a black > green > yellow color scale, representing values (0.0 > 0.5 > 1.0). A C/T value of 1 for a specific cell type has been derived from a set of training data for each cell type or tissue.[7] Using this approach, 20 cell types can be distinguished, including those from ESCs; ovary, testis, neurons, glia, skin, heart, skeletal muscle, fibroblasts, white adipose, kidney, endothelial cells, hematopoietic stem and progenitor cells (hspc), B cells, T cells, macrophages, lung, liver, pancreas, small intestine, and colon. The C/T GRNs score for each different cell type is based on GRNs, specific to each cell type. Thus, a given GRN is associated with a particular cell or tissue type. The values in the bar blots in Figure 3B represent the extent of similarity between undifferentiated and differentiated ESCs for C/T GRN for these 20 different cell types. As indicated in Figure 3, the undifferentiated SCR ESCs and the 4-day-old EBs could be clearly distinguished from the 8-, 12-, and 16-day-old EBs. The C/T score was relatively high for undifferentiated SCR ESCs (close to 1), as well as for early differentiation stages in 4-day-old SCR EBs (scores close to 0.5), but very low for the 8-, 12-, and 16-day-old EBs (Figure 3A). Based on their GRN score status, we could distinguish ESCs, heart, fibroblasts, hspc, macrophages, lung, and liver cells (Figure 3B). As indicated in Figure 3B, maximal GRN scores for skin, hspc, macrophage, fibroblast, heart, and liver were overrepresented in 16-day, 8-day, 12-day, 12-day, 12-day, and 16-day-old EBs, respectively. All three independent experiments showed similar tendencies (Figure 3). Similar results were obtained for WT ESCs (Figure S3). In contrast, the KD ESCs, as well as their 4-, 8-, 12-, and the 16-day-old KD EBs had high scores (close to 1), typical for undifferentiated ESCs (Figure 4). No other somatic cell types could be distinguished by its C/T score.

These findings again suggest perturbation of the differentiation processes of Strip2 deficient ESC toward somatic cells.

MicroRNA Gene Expression Analysis

Next, we determined the global expression profile for miRNAs during the differentiation of WT, SCR, and KD ESCs, using Affymetrix microRNA 3.0 arrays, as described previously.[8] Figure 5 shows a PCA plot of these expression levels. Significance of the variances of these expression levels was evaluated using PCA. PC1 showed the highest variance in miRNA transcriptomes of these samples, followed by PC2. The miRNA transcriptomes of 4-day-old SCR and WT EBs were very similar and showed clear differences in PC1 and PC2, compared with other differentiation stages. The transcriptomes of the 8-, 12-, and 16-day-old WT, as well as SCR EBs were similar, characterized by small differences in PC2. The transcriptomes of the 4-, 8-, 12-, and 16-day-old KD EBs were similar to undifferentiated KD, SCR, and WT ESCs in PC1, with minor differences in PC2. Clusters containing miRNAs that were similarly regulated during differentiation of the KD, SCR, and WT ESCs are shown in Figure 5B (a representative time course of expression levels of different miRNAs clusters in differentiated WT and KD ESCs is shown in Figure 5C). As shown in Figure S1B, the expression levels of the miRNAs in differentiated SCR ESCs were very similar to the expression levels in the differentiated SCR ESCs. Of particular interest were clusters 1 and 4, with miRNAs belonging to the let-7 family,

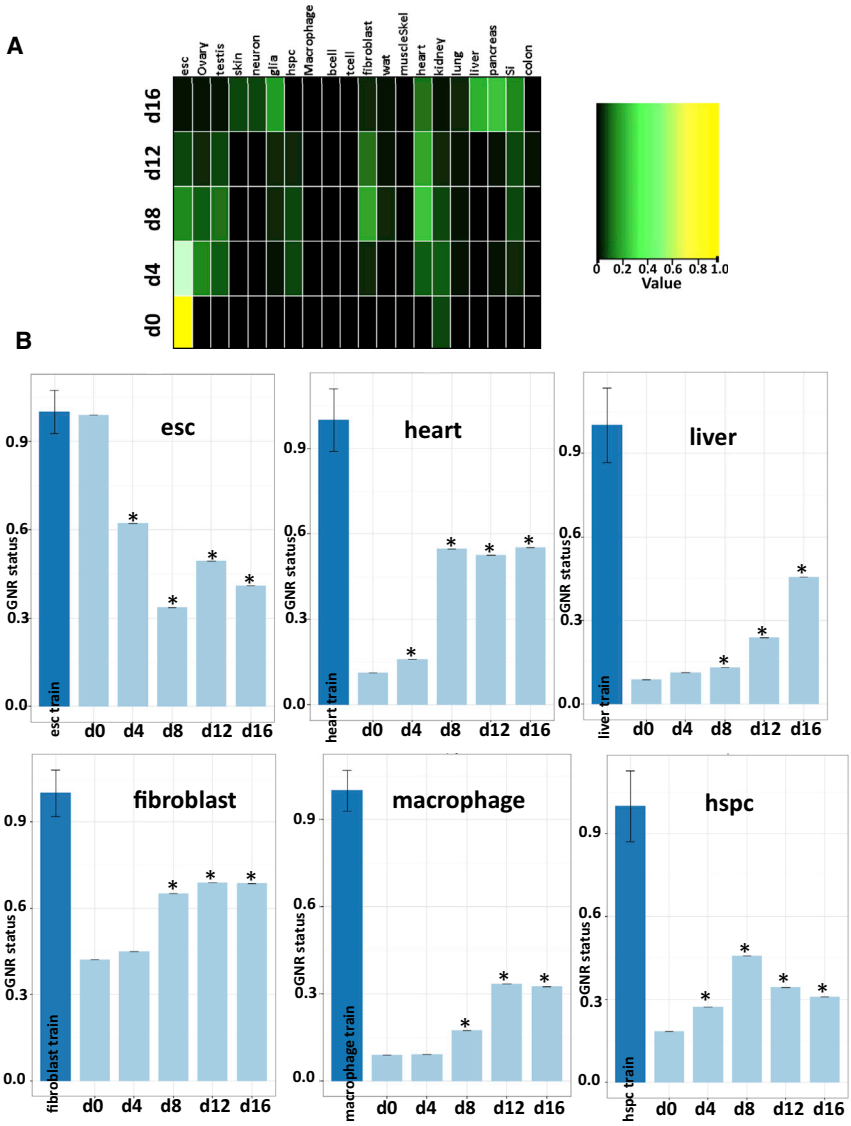

Figure 3. CellNet Analysis of Differentiated SCR ESCs
Gene expression .CEL files from the undifferentiated control SCR ESCs, as well as from 4-, 8-, 12-, and 16-day-old EBs were analyzed using online CellNet bioinformatics tool (http://cellnet.hms.harvard.edu/run/). (A) C/T classification score. (B) C/T gene regulatory network (GRN) status score (*$p < 0.05$ for differentiated SCR ESCs versus undifferentiated SCR ESCs, mean ± SEM).

as well as clusters 5 and 9 having miRNAs belonging to the 290 and 302 miRNA families, respectively. Progressive differentiation of ESCs correlated well with high levels of expression of Let-7d, Let-7c, and Let-7e (Figure 6A). A pronounced expression of let-7 miRNAs in WT and SCR ESCs began on day 12 and remained very high after 16 days of differentiation. In contrast, the expression of let-7 miRNAs in differentiated KD ESCs remained extremely low during differentiation (Figure 6B). Meanwhile, the expression levels of 290 family miRNAs were very high in undifferentiated ESCs, but expression levels decreased with progressive differentiation (Figure 6B). In contrast to KD EBs having very low expression levels of 302 miRNAs, their expression was maximal in 4-day-old SCR and WT EBs (Figure 6C). These findings suggest perturbation of the miRNAs expression in Strip2 deficient ESCs essential for the differentiation of ESCs.

Enzymatic Assay of the Activity of Epigenetic Regulators in the Nuclei of Differentiated ESCs

Of particular interest was our observation that the gene expression levels of *Dnmt3b* and *Hat1* remained high during the differentiation of KD ESCs. Therefore, we further investigated the nuclear and cytosolic activity of Hat1 and Dnmt3b in KD and SCR ESCs, as well as in their 4- and 16-day-old differentiated EBs. As expected, with increasing differentiation of SCR ESCs, the DNA methylation occurring in the nucleus significantly decreased (Figure 7A). In contrast, the DNA methylation remained high in 4- and 16-day-old KD EBs, being significantly higher than 4- and 16-day-old SCR EBs (Figure 7A). Hat1 activity was similarly investigated. Because Hat1 has been found in both nucleus and cytoplasm,[9] we checked its activity in both the cytosol and the nucleus. Hat1 activity was reduced in 4- and 16-day-old EBs, but had significantly higher activities in KD EBs, compared with SCR EBs. The cytosolic Hat1 activity in undifferentiated SCR ESCs and in 4-day-old SCR EBs was very similar, but was significantly lower on day 16 of differentiation (Figure 7B). In contrast, the activity of the Hat1 in 4- and 16-day-old KD EBs was significantly higher than in 4- and 16-day-old SCR EBs (Figure 7B). These findings suggest that the elevated gene expression of *Dnmt3b* and *Hat1* in differentiated KD ESCs correlates well with the increased enzymatic activity of Hat1 and Dnmt3.

Analysis of the Pluripotent Factors by Immunostaining and Teratoma Formation Assay of the 16-Day Differentiated Strip2-Silenced ESCs

Because pluripotent factor genes were highly upregulated in differentiated KD ESCs, even after a 16-day differentiation period, we analyzed the expression of these pluripotent factors on a protein level using immunostaining. As expected, Oct4, Sox2, and Nanog were present in undifferentiated WT ESCs, but were completely absent in 16-day-old differentiated WT ESCs. In contrast, all three pluripotent factors were expressed in 16-day-old KD EBs (Figure S4A). In addition, we validated the teratoma formation of the undifferentiated 16-day KD

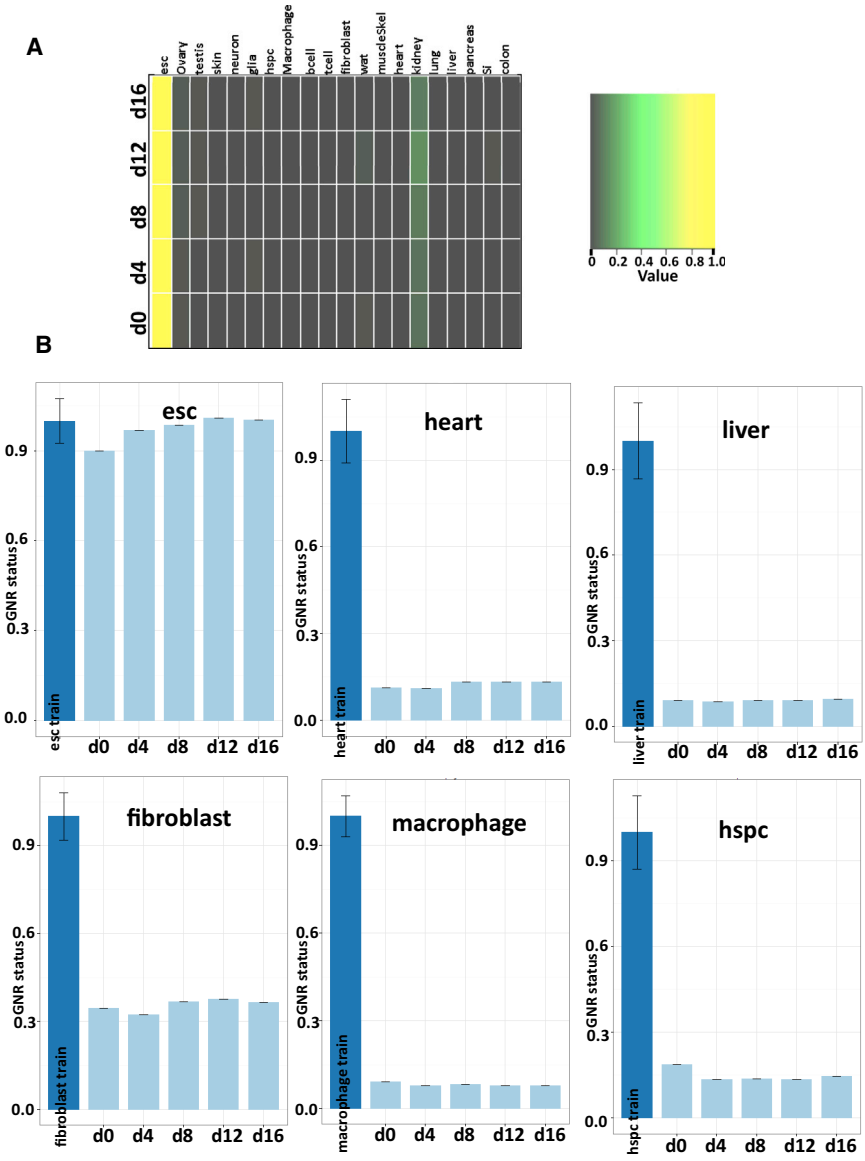

Figure 4. CellNet Analysis of Differentiated KD ESCs
Gene expression .CEL files from the undifferentiated Strip2-silenced KD ESCs, as well as 4-, 8-, 12-, and 16-day EBs were analyzed using online CellNet bioinformatics tools (http://cellnet.hms.harvard.edu/run/). (A) C/T classification score. (B) C/T gene regulatory network (GRN) status scores.

and SCR EBs (Figure S4B). In contrast to cells from the 16-day-old SCR EBs, subcutaneous injections of the dissociated 16-day-old KD EBs in severe combined immunodeficient (SCID) mice resulted in formation of huge tumors. These results suggest a high tumorigenicity potential of the Strip2 deficient 16-days differentiated ESCs.

DISCUSSION

To determine the role of Strip2 in cell differentiation, we previously silenced Strip2 in ESCs and investigated its role in their differentiation. Using transcriptomic microarray studies, we were able to demonstrate that Strip2 is essential for differentiation of ESCs into different cell types. In addition, *Strip2* encodes for a protein having a molecular weight of 96 kDa, which is typically located in the nucleoli of undifferentiated ESCs.[6] In contrast, in undifferentiated ESCs, Strip2 was mainly distributed perinuclear or within the nucleus. In differentiated cells at day 16, it occurs in specific differentiated cell types. These findings indicated that Strip2 is highly expressed in some specific somatic cells, whereas in others, it is marginally expressed. This observation is in agreement with in vivo experiments that show Strip2 is preferably expressed in the heart and brain.[10,11] Thus, Strip2 was mainly detected in the nuclear bodies of the Strip2-expressing differentiated cells. In general, these nuclear bodies are membrane-less organelles, which can be categorized into nucleoli, Cajal bodies, promyelocytic leukemia nuclear bodies, polycomb bodies, and others.[12] Although the functions of these nuclear bodies is not completely known, in coordination with ncRNAs and other chromatin modifiers, they have been shown to be involved in: (1) processing of RNAs, including ncRNAs; (2) the assembly of ribonucleoprotein complexes; and (3) epigenetic regulation of gene expression.[12] Using transcriptomics, our previous study dealing with undifferentiated ESCs and 12-day-old EBs provided evidence that Strip2 was essential for the differentiation of ESCs into somatic cells.[6] In addition, Strip2 may be required for the development of germ layers from ESCs or in the development of somatic cells from germ layer cells. To answer this question, we extended our transcriptome studies through performing a narrow time window differentiation of KD, SCR, and WT ESCs and carrying out detailed parallel transcriptome and miRNA analyses. The results obtained in this study indicate that pluripotent transcriptional factors were highly upregulated at all stages of differentiation of the KD ESCs. Accordingly, the tumorigenic potential of the 16-day-old KD EBs was very high, compared with differentiated 16-day-old SCR EBs. Our transcriptome findings demonstrate that expression of the germ layers (ectoderm, endoderm, and mesoderm) and formation of specific genes that were maximally expressed in 4-day-old SCR and WT EBs were completely inhibited during all stages of differentiation of KD ESCs, including their 4-day-old EBs. Our findings also show a maximal expression of genes in 4-day-old EBs, regulating the formation of germ layers (Table 1). These findings and the CellNet analysis demonstrate that Strip2 acts very early on the differentiation

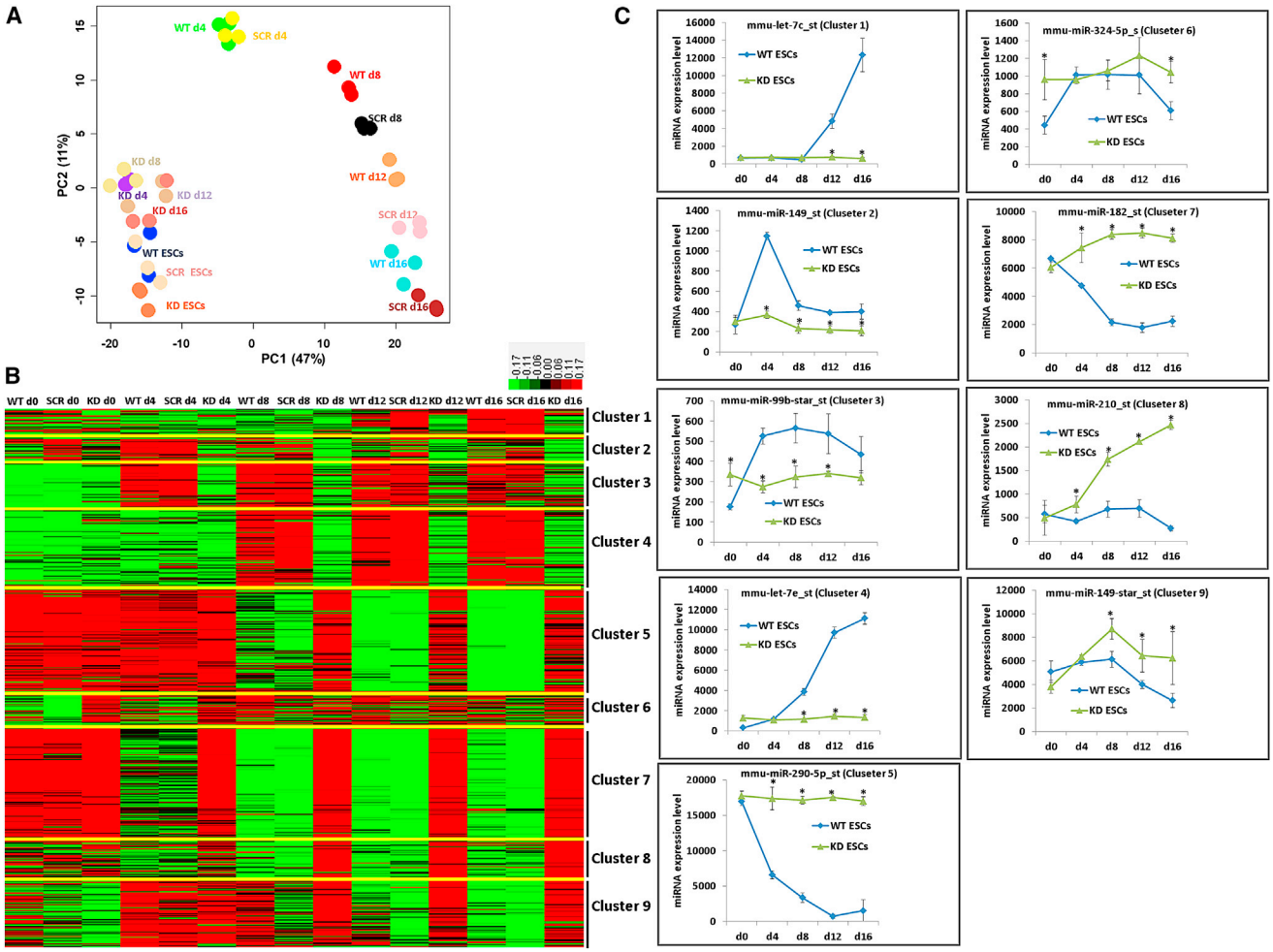

Figure 5. MicroRNA Analysis of Strip2-Silenced KD, SCR, and WT ESCs

Differentiation of these cells was performed for 4-, 8-, 12-, and 16-day periods. (A) PCA of microRNA expression. Each sphere represents an individual sample from a color-coded triplicate sample set. (B) Visualization of nine clusters of miRNAs, each indicating expressed miRNAs having similar levels of expression at different stages of differentiation. The means of the three replicates are displayed on the vertical axis, with genes on the horizontal axis. Log2 transformed signal intensities are depicted using a color gradient. The heatmap indicates high expression levels in red, intermediate expression in dark gray, and low expression levels in green. (C) Representative plots show representative gene expression levels for specific clusters.

process, and its presence in ESCs is indispensable for the initiation of differentiation toward the formation of germ layer cells and their lineages. From the observation that 4,075 genes were statistically differentially expressed in KD d4, d8, d12, and d16 in comparison to KD ESCs (KD d0) and from the DAVID analysis of these genes (data not shown), we may assume that the differentiation process of the Strip2 deficient ESCs is not completely blocked. Also, based on the GRN score status, the kidney developmental process in differentiated KD ESCs is delayed, but it is not blocked, whereas formation of other somatic cells (Figure 3) and neurons (Figure S5) at day 16 is completely blocked. The results derived from ESCs suggest that not only the process of cardiomyogenesis, but also other processes, such as neurogenesis or hepatogenesis are dependent on the availability of Strip2. Using morpholino-mediated knockdown, we demonstrated that knock down of Strip2 resulted in abnormalities of the heart and vasculature development. However, we did not look specifically for defects of other organs such as brain and liver.[6] More recently, we performed gene expression microarrays studies using RNA from developing mouse heart at stages E10.5 to E19.5 (unpublished data). Its expression gradually increased, reaching a plateau at stage E15.5 (data not shown), suggesting an involvement of Strip2 in progressive development of the heart.

The CpG DNA methylation status in the nucleus is mediated by CpG methyltransferases, Dnmt3a, Dnmt3b, as well as Dnmt1 and is very highly expressed in undifferentiated ESCs and iPSCs.[6,13] Consistent with these results, we found high expression values of *Dnmts* in all stages of differentiation of ESCs, as well as high enzymatic activity of Dnmt3b in KD ESCs, even after 16 days of differentiation. There is strong evidence that histone modifications in the ESC genome,

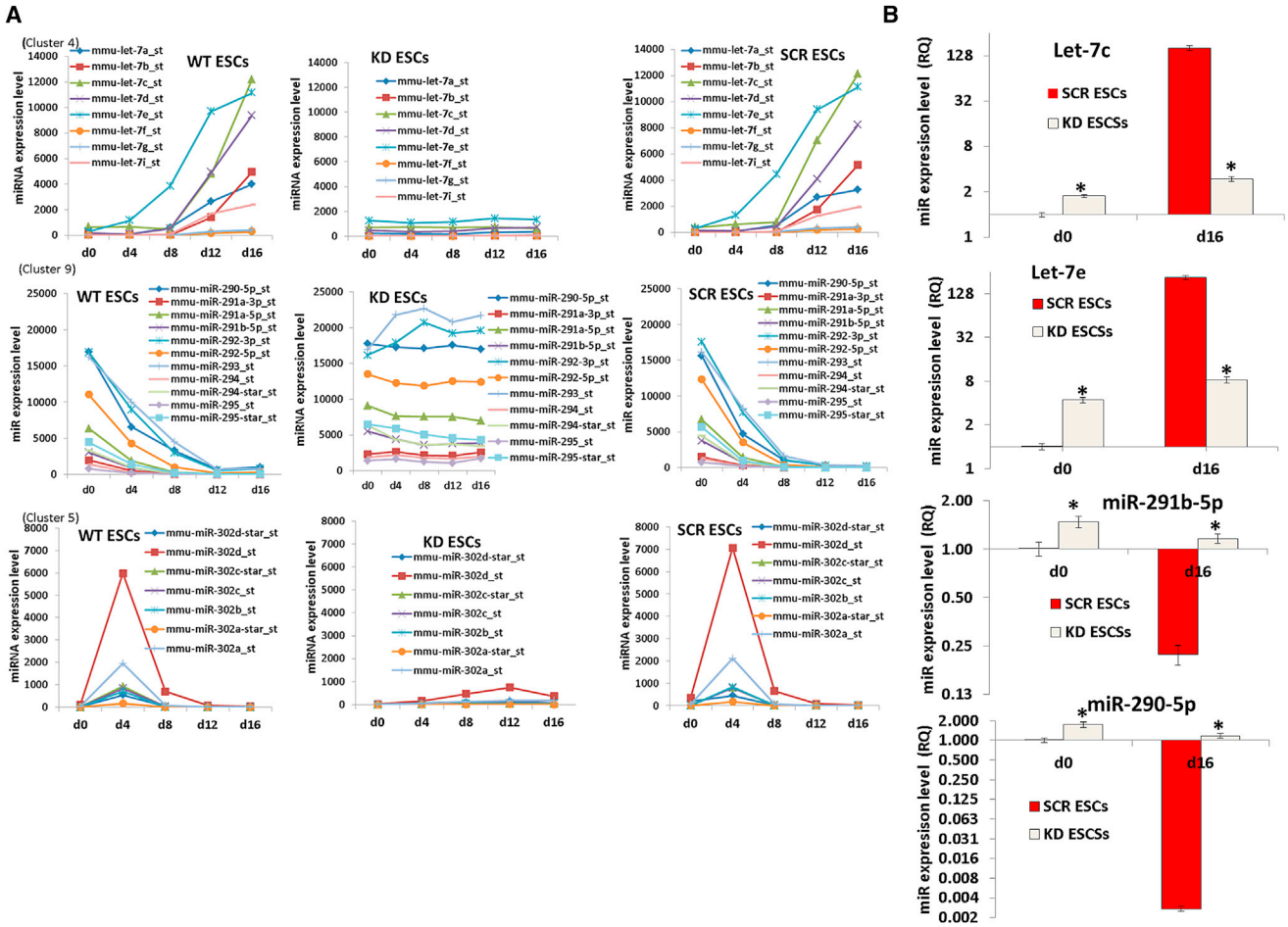

Figure 6. Expression of the MicroRNAs, let-7, 290, and 302 Family MicroRNAs in Differentiated Strip2-Silenced KD, Control SCR, and WT ESCs

(A) Microarray analysis of the differentiation of the cells was performed for 4-, 8-, 12-, and 16-day periods. The means of the three replicates are plotted against the differentiation period. (B) Validation of the microRNA microarray data by the real-time qPCR analysis of some representative miRNAs expressed at undifferentiated (d0) and d16 differentiated KD and SCR ESCs (*$p < 0.05$ for undifferentiated KD ESCs or 16-day KD EBs versus undifferentiated SCR ESCs or SCR 16-day EBs, mean ± SD n = 3). The y axis (logarithmic scale) shows the relative quantification (RQ) of the miRNA expression values as the fold changes to SCR ESCs.

such as acetylation, define its pluripotent status.[14,15] In general, during differentiation of ESCs, histone acetylation decreases.[14–17] Moreover, the expression of *Hat1* was very high at all times during differentiation of KD and SCR ESCs, with significantly higher nuclear Hat1 activity in differentiated 4-day- and 16-day-old KD EBs, compared with differentiated SCR ESCs. Our results are supported from the findings of other groups, demonstrating that the activities of epigenetic regulators, such as Dnmt3b and Hat1, are increased in the pluripotent stadium of ESCs, but decrease during progressive differentiation.[9,13,18]

Numerous miRNAs are key regulators in maintaining pluripotency and differentiation in ESCs.[19,20] Epigenetic modifications of ESCs also help maintain pluripotency and differentiation.[13] Therefore, miRNAs and epigenetic activities in the differentiated ESCs were investigated. Our findings show that elevation of expression in the let-7 family miRNAs correlates well with the period of differentiation of SCR and WT ESCs. Notably, no expression of let-7 miRNAs was observed during differentiation of KD ESCs. These results demonstrate that let-7 family miRNAs are required for differentiation of ESCs and that the nuclear Strip2 in ESCs is required to inhibit expression of let-7 and 302 family miRNAs. In this context, it has been reported that posttranslational methylation of nuclear LIN28A represses let-7 miRNA expression in ESCs by sequestering pri-let-7 in the nucleus. Because it is required for generation of let-7, this prevents differentiation of ESCs.[21]

Interestingly, the expression levels of the 290 to 295 miRNAs in SCR and WT ESCs have opposing behavior during differentiation, having an initially high level in undifferentiated cells, but gradually decreasing during differentiation. Consistently, the 290 to 295 miRNAs are highly expressed in undifferentiated ESCs, but their expression declines upon progressive differentiation (see extensive review Rosa and Brivanlou[22]). In contrast, in differentiated KD ESCs, their expression levels

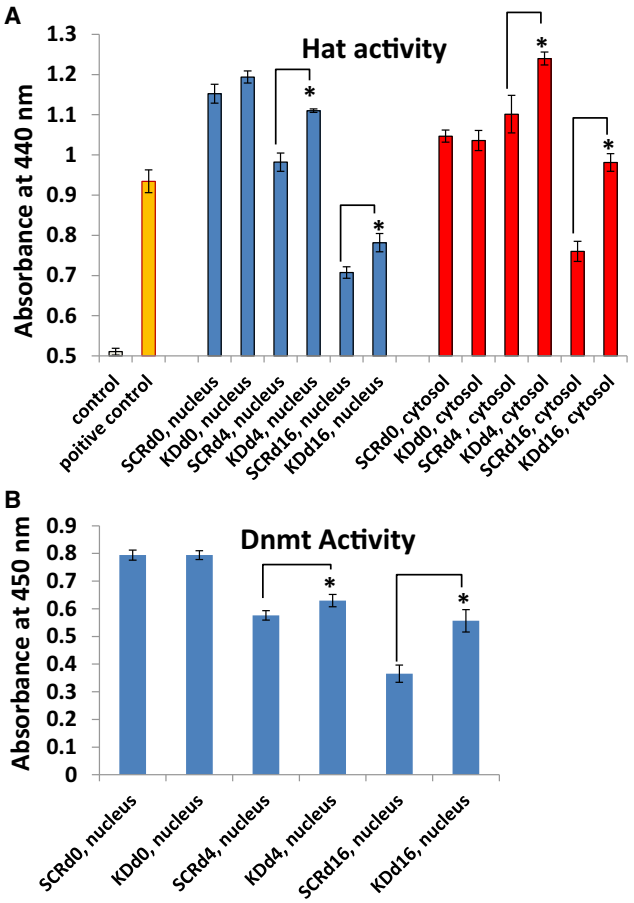

Figure 7. Activity of the Hat and Dnmt in Undifferentiated and Differentiated Strip2-Silenced KD and Control SCR ESCs

(A and B) After isolation of the nuclei and cytosolic fractions, the relative Hat (A) or Dnmt (B; CpG methyltransferase) activity was measured by colorimetric assays at an absorbance at 440 nm or 450 nm, respectively (*$p < 0.05$; mean ± SD; n = 3, independent experiments).

remain as high as in undifferentiated KD ESCs. It has been reported that the 302 family miRNA members are highly upregulated in undifferentiated ESCs, but less expressed in differentiated cells for review see Rosa and Brivanlou[22] and Jouneau et al.[23]). According to our findings, miRNAs of the 302 family are lowly expressed in undifferentiated WT and SCR ESCs, with maximal expression occurring in 4-day-old EBs and expression rapidly decreasing onward of day 8 of differentiation. Again, the expression of the 302 family miRNAs remains low during all stages of differentiation in KD ESCs, including their 4-day-old EBs. In summary, our results demonstrate that Strip2 is a nuclear factor that has an indispensable role in the differentiation of ESCs.

MATERIALS AND METHODS

Culturing and Differentiation Assays of ESCs

The loss-of-function experiments were performed with murine CGR8 ESC from the European Collection of Cell Cultures (ECACC; No. 95011018). The cells were maintained on (0.2%) gelatinized tissue-culture dishes under feeder-free conditions in a standard ESC culture medium, consisting of Glasgow's minimum essential medium (GMEM; Invitrogen), supplemented with 10% fetal bovine serum (FBS; GIBCO, Thermo Fisher Scientific,), 2 mM L-glutamine, 100 units/mL leukemia inhibitory factor (LIF-1; Calbiochem), and 50 μM β-mercaptoethanol (β-ME; Invitrogen), as described previously.[24] The cells were passaged on alternate days and maintained confluence between 60%–70%. ESC differentiation was inducted by the conventional "hanging drop" protocol, as described previously.[24] Briefly, 20-μL hanging drops were made in 10-cm diameter low adhesion dishes from a trypsin-dissociated ESC suspension (2.5×10^4 cells/mL), prepared in differentiation medium (Iscove's modified Dulbecco's Medium, IMDM; Life Technologies), supplemented with 20% fetal calf serum, 1% non-essential amino acids, 2 mM L-glutamine, and 100 μM β-ME. Plates were incubated at 37°C, under 5% CO_2 in a humidified incubator for 2 days. EBs formed were harvested by washing and were resuspended in differentiation medium. The EBs were incubated at 37°C under 5% CO_2 in an incubator under shaking conditions, with a medium change on alternate days. EBs were monitored for beating areas, called cardiomyocyte foci, starting from day 7 after differentiation, using an inverted phase contrast microscope (Axiovert25; Zeiss). The numbers of beating EBs were counted and representative videos were captured (Sony DFW-X700, Sony).

Transfection of Vectors into Undifferentiated ESCs and Generation of a Constitutive Strip2-Silenced ESC Line

The shRNA expression vector pGFP-V-RS, targeting mouse Strip2 (TR508344A plasmid) and the scrambled plasmid (TR30013) were purchased from OriGene. The shStrip2 target sequence on its mRNA was 5′ GCAAGACACTAAGGAATGGCTGGAGTTGG 3′, which corresponds to nucleotides 365–393. The scrambled plasmid (TR30013) contains a non-active scrambled sequence cassette (5′ GCACTACCAGAGCTAACTCAGATAGTACT3′). The pGFP-V-RS control, the shRNA vector (TR508344A plasmid), and the scramble shRNA vector (TR30013) were linearized. Generation of the cell lines was performed, as described previously.[6] Briefly, 25 μg of linearized vector was transfected into 10^6 CGR8 cells, suspended in phosphate-buffered saline (PBS), free of Ca^{2+} and Mg^{2+} salts, using a Bio-Rad Gene Pulser Electroporation System (Bio-Rad). The electroporation conditions were 500 μF and 240 V, as described previously.[25] The electroporated cells were cultivated on gelatinized tissue culture flasks for 2 days and eventually selected for treatment with 2 μg/mL puromycin. On day 10 of selection, green fluorescence was monitored under a blue excitation light through a fluorescence microscope. Afterward, the resistant clones were picked for further experiments and amplified following standard ESCs culture conditions. The clones were passaged at least four times before being used in experiments to attain a stable gene expression profile. The shStrip2 cell line generated with the TR508344A plasmid was used to study gene expression changes during differentiation of EBs.

Microarray Analysis

Total RNA was isolated from the 12-day-old KD EBs, 12-day-old SCR EBs, and WT undifferentiated ESCs, using an RNeasy Mini Kit

(QIAGEN). Aliquots containing 100 ng total RNA were used for amplified (a)RNA amplification with GeneChip 3′ IVT Express Kit (Affymetrix, Thermo Fisher Scientific). After 16 hr of biotinylated in vitro transcription, the aRNA was purified. Next, 15 μg of purified aRNA was fragmented with fragmentation buffer. Another 12.5 μg of fragmented aRNA was hybridized with Mouse Genome 430 2.0 arrays for 16 hr at 45°C. Arrays were washed and stained with phycoerythrin using Affymetrix Fluidics Station 450 and scanned using the Affymetrix GeneChip Scanner 3000 7G. The quality control matrices were confirmed using Affymetrix GCOS software version 1.3. The raw data were background corrected and normalized using a robust multi-array averaging algorithm, executed by R Bioconductor packages.[26] A PCA was performed to evaluate samples transcriptome variability. Significantly regulated transcripts were determined using an empirical Bayes linear model, applied using the LIMMA package in R.[27] The significance of expression changes were calculated, correcting the p value of the t-score for a false discovery rate using the Benjamini-Hochberg method with $p \leq 0.05$. The size of each change was calculated, with a 2-fold change threshold. On significantly expressed values, K-means clustering analysis was performed, after normalization of signal values (mean = 0 and SD = 1), using Euclidian distance measurement and k = 5 in Cluster 3.0.[28] The microarray data have been deposited in the Gene Expression Omnibus (GEO) (NCBI): GSE96809.

CellNet and Gene Ontology and Pathway Analysis

CellNet analysis was performed using online bioinformatics tools (http://cellnet.hms.harvard.edu/run/, as described previously.[7] To determine the biological significance of differentially expressed transcripts (DETs), the database DAVID v6.8 was used (https://david.ncifcrf.gov/). DAVID provides biological process, molecular function, and cellular component for DETs having an Expression Analysis Systematic Explorer (EASE) enrichment score with $p \leq 0.01$.[29,30]

Real-Time Quantification PCR

For the real-time qPCR and miRNA validation, RNAs extracted for the microarray experiment were utilized. For real-time qPCR, 1 μg total RNA was used for synthesis of cDNA along with SuperScript Vilo cDNA synthesis kit (Invitrogen) in compliance with instructions provided on the kit. There were 100 ng of the synthesized cDNA that was used for real-time qPCR analysis. The primer sequences were derived from primer bank (https://pga.mgh.harvard.edu/primerbank/) and have been listed in the Table S3. Platinum SYBR Green qPCR SuperMix (Invitrogen) was used with the Applied Biosystems 7500 Fast cycler. The expression of target genes was normalized to reference gene GAPDH. The mRNA expression values were represented as fold change relative to SCR ESCs. For the miRNA validation, 1 μg of total RNA was used to synthesize cDNA using miScript II RT Kit (QIAGEN), according to the kits instructions. There were 100 ng of synthesized cDNA that was used for miRNA assay. The miRNA primers were purchased from QIAGEN and information including catalog no are listed in the Table S3. miScript SYBR Green PCR Kit (QIAGEN) was used along with Applied Biosystems 7500 standard cycler. The miRNA expression of target genes was normalized to reference gene Hs_SNORD68 (QIAGEN). The relative quantification (RQ) of the miRNA expression values were represented as the fold change to SCR ESCs.

Immunohistochemistry

Cells were fixed with 4% paraformaldehyde in phosphate buffered saline (PBS) (10 mM sodium phosphate, 2.7 mM KCl, 140 mM NaCl, and pH 7.4) for 15 min and then permeabilized with 0.4% Triton X-100, diluted in blocking buffer (5% bovine serum albumin, diluted in PBS) for 15 min at room temperature (RT). After washing the cells three times with PBS for 5 min each time, and blocking them for 45 min at RT, the cells were incubated for 1 hr at RT, with the appropriate antibodies against Oct4, Sox2, Nanog, and polyclonal Strip2 antibodies (sc-162799; Santa Cruz Biotechnology), diluted to 1:200 in blocking buffer. Excessive antibodies were washed off with PBS and cells were incubated for 1 hr with donkey anti goat IgG-FITC secondary antibody (sc-2024; Santa Cruz Biotechnology), diluted to 1:200 in blocking buffer. Cells were again washed thrice with PBS for 5 min each time. To visualize the nucleus, the cells were incubated for 1 hr with Hoechst 33342 (Life Technologies), diluted to 1:1,000 in blocking buffer. After the final wash, the cells were fixed on microscopic slides with PolyGlass coverslip medium (Polysciences). Images were captured with an inverted fluorescence microscope (Zeiss Axiovert 200) or, for higher subcellular resolution of nuclei and nucleoli, with an Olympus FluoView1000 confocal system (Olympus), as described previously.[6] Immunostaining of the pluripotent factors in 16-day EBs has been performed as descripted previously.[31] Briefly, 16-day EBs were fixed using 4% paraformaldehyde at room temperature, washed with PBS, and embedded in Tissue Tek OCT (Sakura Finetek Japan, http://www.sakura-finetek.com/). After cryoslicing (8 μm), cryosections were placed on silanized slides. Immunostaining of the pluripotent factors Oct4, Nanog, and Sox2 and staining of the nuclei has been performed as indicated above.

Hat Colorimetric Assay Activity

Hat enzymatic activity in undifferentiated SCR and KD ESCs, as well as in differentiated 4-, and 16-day SCR and KD EBs was determined at the nuclear and cytosolic fraction. Fractionation of the nuclei and cytosol has been performed according to the BioVision kit (product number: K266-25) (BioVision) of 10^6 cells after trypsinization of the undifferentiated and 16-day EBs. The Hat activity has been determined in a 96-well plate according to the Hat activity colorimetric assay kit from BioVision (K332-100). According to the instructions of the kit manual, the kit utilizes active nuclear extract from HeLa cells as a positive control and acetyl CoA as a co-factor. Acetylation of a supplied peptide substrate by active Hat releases the free form of CoA, which is a co-enzyme for producing NADH. NADH reacts with a soluble tetrazolium dye, and the reaction product can be detected by the absorption at 440 nm.

Dnmt Activity/Inhibition Assay Activity

The DNMT activity of the nuclear fractions of 10^6 cells has been determined using the DNMT Activity/Inhibition Assay from Active

Motive (product number: 55006) an ELISA-based method as described in the company manual and previously.[32] According to the manual, a CpG-enriched DNA substrate has been immobilized on a 96-stripwell plate, and nuclear extracts with high DNMT activity catalyze the transfer of methyl groups from the provided AdoMet reagent to the coated DNA substrate. The resulting methylated DNA is recognized by the His-tagged recombinant MBD2b pending on the enzymatic activity of Dnmt. Finally, determination of the Dnmt activity occurred by the addition of a poly-histidine antibody conjugated to horseradish peroxidase (HRP) and by measuring the absorbance at 450 nm.

Teratoma Analysis

The teratoma assay was performed on SCID (Rag2^{-}/$^{-}$common gamma^{-}/$^{-}$) mice, as described previously.[33] The animal experiments have been approved by the Universitätsklinikum Köln (Institutional Ethics Review Board reference number 01-090) and the governmental animal care and use office (Landesamt für Natur, Umwelt und Verbraucherschutz Nordrhein- Westfalen, Recklinghausen, Germany (reference number 84-02.04.2012.A417 LANUV). Briefly, 16-day-old EBs derived from KD and SCR ESC lines were dissociated with trypsin, and 10^6 single cells in 200 µL DMEM were injected subcutaneously into the dorsal flanks of SCID (Rag2^{-}/$^{-}$common gamma^{-}/$^{-}$) mice. KD and SCR ESCs (10^6 cells each; in 200 µL DMEM) were also subcutaneously injected into SCID mice, as controls. At 4 weeks after these injections, tumors were dissected from the mice. Samples were fixed in PBS containing 4% paraformaldehyde and embedded in paraffin. Tissue sections were stained with hematoxylin and eosin.

Statistical Analysis

If not otherwise indicated in the text, then analysis was performed using a one-way pairwise ANOVA test, and p values < 0.05 were considered to be statistically significant.

SUPPLEMENTAL INFORMATION

Supplemental Information includes five figures and three tables and can be found with this article online at http://dx.doi.org/10.1016/j.omtm.2017.04.001.

AUTHOR CONTRIBUTIONS

D.S. performed the cell culturing experiments and coordinated the experiment. S.R. performed the microarray experiments; and D.P. performed the enzymatic activity assay. J.A.G. performed the analysis of the microarray data. D.S. and S.R. performed the immunostaining experiments; M.A.A. and S.P. performed the confocal imaging and microscopy. S.P.S. and A.S. performed the CellNet analysis of the microarray data. V.W., M.X.D., and J.H. contributed to the editing of the manuscript. N.R., H.A., and D.S. performed the teratoma assay. A.S. supervised the study, interpreted the results, and wrote the manuscript.

CONFLICTS OF INTEREST

The authors declare no conflict of interest.

ACKNOWLEDGMENTS

This work was supported by German Research Foundation (DFG) grant SA 568/17-2 to A.S.

REFERENCES

1. Bai, S.W., Herrera-Abreu, M.T., Rohn, J.L., Racine, V., Tajadura, V., Suryavanshi, N., Bechtel, S., Wiemann, S., Baum, B., and Ridley, A.J. (2011). Identification and characterization of a set of conserved and new regulators of cytoskeletal organization, cell morphology and migration. BMC Biol. *9*, 54.

2. Goudreault, M., D'Ambrosio, L.M., Kean, M.J., Mullin, M.J., Larsen, B.G., Sanchez, A., Chaudhry, S., Chen, G.I., Sicheri, F., Nesvizhskii, A.I., et al. (2009). A PP2A phosphatase high density interaction network identifies a novel striatin-interacting phosphatase and kinase complex linked to the cerebral cavernous malformation 3 (CCM3) protein. Mol. Cell. Proteomics *8*, 157–171.

3. Hwang, J., and Pallas, D.C. (2014). STRIPAK complexes: structure, biological function, and involvement in human diseases. Int. J. Biochem. Cell Biol. *47*, 118–148.

4. Shi, Z., Jiao, S., and Zhou, Z. (2016). STRIPAK complexes in cell signaling and cancer. Oncogene *35*, 4549–4557.

5. Madsen, C.D., Hooper, S., Tozluoglu, M., Bruckbauer, A., Fletcher, G., Erler, J.T., Bates, P.A., Thompson, B., and Sahai, E. (2015). STRIPAK components determine mode of cancer cell migration and metastasis. Nat. Cell Biol. *17*, 68–80.

6. Wagh, V., Doss, M.X., Sabour, D., Niemann, R., Meganathan, K., Jagtap, S., Gaspar, J.A., Ardestani, M.A., Papadopoulos, S., Gajewski, M., et al. (2014). Fam40b is required for lineage commitment of murine embryonic stem cells. Cell Death Dis. *5*, e1320.

7. Cahan, P., Li, H., Morris, S.A., Lummertz da Rocha, E., Daley, G.Q., and Collins, J.J. (2014). CellNet: network biology applied to stem cell engineering. Cell *158*, 903–915.

8. Meganathan, K., Jagtap, S., Srinivasan, S.P., Wagh, V., Hescheler, J., Hengstler, J., Leist, M., and Sachinidis, A. (2015). Neuronal developmental gene and miRNA signatures induced by histone deacetylase inhibitors in human embryonic stem cells. Cell Death Dis. *6*, e1756.

9. Parthun, M.R. (2012). Histone acetyltransferase 1: More than just an enzyme? Biochim. Biophys. Acta *1819*, 256–263.

10. Eden, M., Meder, B., Völkers, M., Poomvanicha, M., Domes, K., Branchereau, M., Marck, P., Will, R., Bernt, A., Rangrez, A., et al.; German Mouse Clinic Consortium (2016). Myoscape controls cardiac calcium cycling and contractility via regulation of L-type calcium channel surface expression. Nat. Commun. *7*, 11317.

11. Wagh, V., Jagtap, S., Meganathan, K., Potta, S.P., Winkler, J., Hescheler, J., and Sachinidis, A. (2012). Effect of chemopreventive agents on differentiation of mouse embryonic stem cells. Front Biosci. *4*, 156–168.

12. Mao, Y.S., Zhang, B., and Spector, D.L. (2011). Biogenesis and function of nuclear bodies. Trends Genet. *27*, 295–306.

13. Boland, M.J., Nazor, K.L., and Loring, J.F. (2014). Epigenetic regulation of pluripotency and differentiation. Circ. Res. *115*, 311–324.

14. Kim, M.S., Cho, H.I., Park, S.H., Kim, J.H., Chai, Y.G., and Jang, Y.K. (2015). The histone acetyltransferase Myst2 regulates Nanog expression, and is involved in maintaining pluripotency and self-renewal of embryonic stem cells. FEBS Lett. *589*, 941–950.

15. Young, R.A. (2011). Control of the embryonic stem cell state. Cell *144*, 940–954.

16. Kobayakawa, S., Miike, K., Nakao, M., and Abe, K. (2007). Dynamic changes in the epigenomic state and nuclear organization of differentiating mouse embryonic stem cells. Genes Cells *12*, 447–460.

17. Meshorer, E., and Misteli, T. (2006). Chromatin in pluripotent embryonic stem cells and differentiation. Nat. Rev. Mol. Cell Biol. *7*, 540–546.

18. Tee, W.W., and Reinberg, D. (2014). Chromatin features and the epigenetic regulation of pluripotency states in ESCs. Development *141*, 2376–2390.

19. Ivey, K.N., and Srivastava, D. (2010). MicroRNAs as regulators of differentiation and cell fate decisions. Cell Stem Cell *7*, 36–41.

20. Ivey, K.N., and Srivastava, D. (2015). microRNAs as developmental regulators. Cold Spring Harb. Perspect. Biol. *7*, a008144.

21. Kim, S.K., Lee, H., Han, K., Kim, S.C., Choi, Y., Park, S.W., Bak, G., Lee, Y., Choi, J.K., Kim, T.K., et al. (2014). SET7/9 methylation of the pluripotency factor LIN28A is a nucleolar localization mechanism that blocks let-7 biogenesis in human ESCs. Cell Stem Cell *15*, 735–749.

22. Rosa, A., and Brivanlou, A.H. (2013). Regulatory non-coding RNAs in pluripotent stem cells. Int. J. Mol. Sci. *14*, 14346–14373.

23. Jouneau, A., Ciaudo, C., Sismeiro, O., Brochard, V., Jouneau, L., Vandormael-Pournin, S., Coppée, J.Y., Zhou, Q., Heard, E., Antoniewski, C., and Cohen-Tannoudji, M. (2012). Naive and primed murine pluripotent stem cells have distinct miRNA expression profiles. RNA *18*, 253–264.

24. Gissel, C., Voolstra, C., Doss, M.X., Koehler, C.I., Winkler, J., Hescheler, J., and Sachinidis, A. (2005). An optimized embryonic stem cell model for consistent gene expression and developmental studies: a fundamental study. Thromb. Haemost. *94*, 719–727.

25. Andressen, C., Stöcker, E., Klinz, F.J., Lenka, N., Hescheler, J., Fleischmann, B., Arnhold, S., and Addicks, K. (2001). Nestin-specific green fluorescent protein expression in embryonic stem cell-derived neural precursor cells used for transplantation. Stem Cells *19*, 419–424.

26. Bolstad, B.M., Irizarry, R.A., Astrand, M., and Speed, T.P. (2003). A comparison of normalization methods for high density oligonucleotide array data based on variance and bias. Bioinformatics *19*, 185–193.

27. Smyth, G.K. (2004). Linear models and empirical bayes methods for assessing differential expression in microarray experiments. Stat. Appl. Genet. Mol. Biol. *3*, Article 3.

28. Eisen, M.B., Spellman, P.T., Brown, P.O., and Botstein, D. (1998). Cluster analysis and display of genome-wide expression patterns. Proc. Natl. Acad. Sci. USA *95*, 14863–14868.

29. Dennis, G., Jr., Sherman, B.T., Hosack, D.A., Yang, J., Gao, W., Lane, H.C., and Lempicki, R.A. (2003). DAVID: Database for annotation, visualization, and integrated discovery. Genome Biol. *4*, 3.

30. Hosack, D.A., Dennis, G., Jr., Sherman, B.T., Lane, H.C., and Lempicki, R.A. (2003). Identifying biological themes within lists of genes with EASE. Genome Biol. *4*, R70.

31. Xi, J., Khalil, M., Spitkovsky, D., Hannes, T., Pfannkuche, K., Bloch, W., Sarić, T., Brockmeier, K., Hescheler, J., and Pillekamp, F. (2011). Fibroblasts support functional integration of purified embryonic stem cell-derived cardiomyocytes into avital myocardial tissue. Stem Cells Dev. *20*, 821–830.

32. Shen, Y., Takahashi, M., Byun, H.M., Link, A., Sharma, N., Balaguer, F., Leung, H.C., Boland, C.R., and Goel, A. (2012). Boswellic acid induces epigenetic alterations by modulating DNA methylation in colorectal cancer cells. Cancer Biol. Ther. *13*, 542–552.

33. Faitschuk, E., Hombach, A.A., Frenzel, L.P., Wendtner, C.M., and Abken, H. (2016). Chimeric antigen receptor T cells targeting Fc µ receptor selectively eliminate CLL cells while sparing healthy B cells. Blood *128*, 1711–1722.